

ENERGY-SAVING TACHOGRAMS OF ACCELERATION (DECELERATION) OF A FREQUENCY-REGULATED ASYNCHRONOUS ENGINE

Purpose. Finding energy-saving speed trajectories in the acceleration and braking modes for a range of supernormal speeds of a short-circuited frequency-regulated asynchronous engine in the acceleration and deceleration regimes as well as examining the total energy losses of this engine in these modes by the example of machine and traction drives.

Methodology. Methods of variational calculus, Runge-Kutta, mathematical interpolation and computer modeling are used.

Findings. Analytic dependencies are obtained for calculating the total energy losses for a frequency-regulated asynchronous engine (FRAE) under conditions of acceleration and deceleration in the range of its super-nominal velocities. A quantitative estimation of these energy losses for a given engine in this speed range is made with respect to the constant and traction loads for the proposed energy-saving and known (linear and parabolic) velocity trajectories. Electromechanical and energy transitional processes in the range of super-nominal speeds for acceleration and deceleration regimes with the traction load were investigated.

Originality. For the first time, an energy-saving (called “quasi-optimal”) trajectory of speed variation at supernormal FRAE speeds is proposed, which allows minimizing the general main engine energy losses in the acceleration and braking modes with constant and traction loads. For the first time, a quantitative estimate of the minimum possible common main losses of this engine in the modes of acceleration and braking in the range of super-nominal velocities for the proposed energy saving velocity trajectory and a comparison of these losses to linear and parabolic tachograms.

Practical value. The use of the obtained results allows reducing unproductive losses of energy in the modes of acceleration and braking of the FRAE at super-nominal speeds with constant and traction loads.

Keywords: *frequency control, asynchronous motor, super-nominal speed, energy saving*

Introduction. Industrial production of frequency-controlled asynchronous engines with increased (more than three times) rotation speed and increased torque (up to two-three times increase compared to its nominal value) are widely used in various branches of agriculture (mechanical engineering, metallurgy, electric transport, etc.). Considering the rise in the electrical energy price observed in Ukraine and all over the world, leads to a decrease in energy losses when operating in the super-nominal speed (SNS) range as being topical in-trend practice.

Literature review. From the analysis of domestic and foreign scientific and technical literature, it has been found that in the majority of well-known publications devoted to the study of the attenuation regimes of the magnetic field of a frequency-regulated asynchronous engine (FRAE), the problem of maximizing its torque is solved. Namely: in [1] – due to the use of a rational algorithm for modulating the output voltage of the inverter supplying the FRAE; in [2] – the choice of the required value of the stator dissipation inductance of the engine; in [3, 4] – by use, respectively, of direct or predictive FRAE vector control. In the rest of the well-known publications, considering the established and transient modes of operation of this engine under SNS, the following are proposed and investigated: in [5] – controlling FRAE at maximum values of its efficiency factor; in [6, 7] – improving the speed of traction FRAE (functioning, as is well known, for the main time in SNS) as applied to electric vehicles and electric trains, respectively; in [8, 9] and article: Haddoun A., Benbouzid M., Diallo D., Abdessemed R., Ghouili J., Srairi K. A Loss-Minimization DTC Scheme for EV Induction Motors, – reduction of

power consumption in traction FRAE, respectively, for the electric train, tram and electric vehicle, achieved when using energy-saving trajectories of their movement. The analysis of these publications suggests that nowadays in the existing scientific and technical literature not enough attention has been paid to the study of the energy saving trajectories of the FRAE under its acceleration and deceleration regimes in the SNS range.

Purpose. The purpose of the article is to find energy-saving speed trajectories for super nominal speeds of a short-circuited FRAE under acceleration and deceleration regimes and to research the total energy losses of this engine in these modes using the example of machine and traction drives.

Results. The following assumptions were made:

- the generally accepted idealized representation of the three-phase FRAE are supplemented by taking into account the power loss in the steel of this engine [10];

- it is proposed to use a vector type of automatic control system (ACS) for an electric drive, which provides separate regulation of the magnetizing I_{1x} and active I_{1y} components (projections) of the generalized vector of the static current \bar{I}_1 (formed by the main harmonic components of the phase stator currents) of the engine on the axis of the rotating orthogonal coordinate system “x–y”, connected by the real axis “x” with the generalized flux linkage vector of the $\bar{\Psi}_r$ FRAE;

- we neglect the free (damped) components of the stator currents in the acceleration and braking modes (which is possible in practice with regard to the use of the vector ACS because of their high speed and accuracy) [8];

- the object of the study for machine and traction electric drives was: acceleration regimes of the FRAE from nominal synchronous ω_n to maximum speed ω_m and electric braking

from maximum ω_m to nominal synchronous speed ω_n to nominal value: $E_{ry} = \omega_{1n} \cdot \Psi_m$ (where Ψ_r and Ψ_m are respectively the current and nominal values of the generalized flux linkage vector of the rotor $\bar{\Psi}_r$, FRAE; ω_1 and ω_{1n} are the current and nominal values of the angular frequencies of motor stator;

- for traction drive, there was no slip between the driving wheels and the road surface;

- FRAE parameters (the active resistances of which were reduced to a temperature of 115 °C) and the values of the inertia moment of the drive J driven to the motor shaft were assumed to be unchanged (presented in Table 1);

- only the main components of the total power losses and the energy of the FRAE, caused by the main (first) harmonic components of the phase stator currents [10]), were considered;

- mathematical dependencies and subsequent calculations are given in the relative system of units common to AC machines [10] (in which the nominal values of the stator frequency ω_{1n} and the rotor synchronous speed ω_n , as is known, are equal to one unit, and the maximum speed ω_m for the considered FRAE, according to Table 1, is $4000/1500 = 2.677$ p. u.).

At the first stage, taking into account the accepted assumptions, we obtain analytical calculated dependences for determining the total main power and energy losses of the FRAE operating in the SNS.

As the initial dependencies for finding the total main power loss (TMPL) ΔP_{en} and the main electromagnetic energy loss (MEEL) ΔW_a and ΔW_d of this engine during acceleration and deceleration, we use the expressions from [10]

$$\Delta P_{en} = (R_s + 0.005 P_n / \eta_n) \cdot I_{1x}^2 + (R_s + 0.005 P_n / \eta_n + k_r^2 R_r) \times \times I_{1y}^2 + \Delta P_{st.n} \cdot \omega_1^2 \cdot (\Psi_m / \Psi_{mn})^2 + \Delta P_{meh.n} \omega^2; \quad (1)$$

$$\Delta W_a = \int_0^{t_a} \Delta P_{en} dt \quad \text{and} \quad \Delta W_d = \int_0^{t_d} \Delta P_{en} dt, \quad (2)$$

in which I_{1x} and I_{1y} are the magnetizing and active projections of the generalized vector \bar{I}_1 of the stator current of the engine,

Table 1

Nominal parameters of the engine and drive

The name of the parameter, measurements	Value	
I Engine AT 250 L4U2:		
power, kW	120	
active line voltage, V	400	
stator frequency, Hz	50	
nominal/maximum speed, rpm	1500/4000	
slip, %	1.5	
torque (M_n), Nm	780	
multiplicity of starting moment	1.8	
multiplicity of the maximum moment	3.5	
coefficient of performance, %	94	
power factor	0.91	
II Machine drive (model 7B-220-6)		
the multiplicity of the static moment (M_r/M_n) during the reverse course of the table	0.2	
given moment of inertia, kg · m ²	3.84	
III Traction drive (model ZIU 582G-012)		
maximal values:	trolley speed, km/h	60
	longitudinal slope, %	8
	the mass of the trolley, t	18.2

created by the first harmonic components of its phase stator currents; Ψ_m and Ψ_{mn} are, respectively, the current and nominal values of the module of the generalized magnetic flux vector $\bar{\Psi}_m$ in the engine air gap; ω_1 is angular frequency of rotation of the magnetic flux of the engine; R_s , R_r and k_r are, respectively, the active resistance of the stator and rotor windings of the FRAE, the coupling coefficient of the engine rotor; P_n and η_n are the nominal values, respectively, of the useful power on the shaft and the efficiency of the engine; $\Delta P_{st.n}$ and $\Delta P_{meh.n}$ are nominal values, respectively, of power losses in steel and mechanical losses of the engine; λ is the coefficient taking into account the dependence of losses in FRAE steel on the frequency ω_1 of changes in the magnetic flux of the engine ($\lambda = 1.3$ [10]); t_a and t_d are the duration of the times of acceleration and braking modes, respectively; t is the current time, counted from the beginning and during the considered modes of acceleration and deceleration: $0 \leq t \leq t_a$ and $0 \leq t \leq t_d$.

Taking into account the known (for example, from the mentioned book by Pivnyak G. G. and others) the calculated dependences for the module I_1 , magnetizing I_{1x} and active I_{1y} projections of the stator current

$$\left. \begin{aligned} I_1 &= (I_{1x}^2 + I_{1y}^2)^{0.5} \\ I_{1x} &= (\Psi_r + T_r \cdot \Psi_r') / L_m, \quad I_{1y} = M / k_r \Psi_r \end{aligned} \right\} \quad (3)$$

(where L_m and $T_r = L_m / k_r R_r$ are, respectively, the inductance of magnetization and the electromagnetic constant of the time of the rotor of the engine) and approximately increasing ratio

$$(\Psi_m / \Psi_{mn})^2 \approx (\Psi_r / \Psi_{rn})^2, \quad (4)$$

we convert the dependence (1) in mind

$$\Delta P_{en} \approx a (\Psi_r + T_r \Psi_r')^2 + b (M^2 / \Psi_r^2) + c \cdot \omega_1^2 \cdot (\Psi_r^2 / \Psi_m^2) + d \cdot \omega^2. \quad (5)$$

In expressions (3–5), the following notation is used: Ψ_r' is the derivative of the modulus of the generalized rotor flux vector over time, M is the electromagnetic moment of the FRAE. The coefficients a , b , c in expression (5) are calculated from the relations

$$\left. \begin{aligned} a &= (R_s + 0.005 P_n / \eta_n) / L_m^2, & d &= \Delta P_{meh.n} \\ b &= (R_s + 0.005 P_n / \eta_n + k_r^2 R_r) / k_r^2, & c &= \Delta P_{st.n} \end{aligned} \right\}$$

Based on the accepted assumption of maintaining the ratios: $\omega_1 \Psi_r = \omega_{1n} \Psi_{rn} = \text{const}$ during acceleration and deceleration of the FRAE in the SNS range, we find for this frequency range $|\omega_1| > \omega_{1n} = 1$ p. u. dependencies for changing the modulus of the rotor flux linkage and its time derivative of the stator's angular frequency

$$\Psi_r = \Psi_m / \omega_1 \quad \text{and} \quad \Psi_r' = -\Psi_m \cdot \omega_1' / \omega_1^2, \quad (6)$$

where ω_1' is the derivative of frequency ω_1 over time.

Taking into account the known relation for the electromagnetic moment [10]

$$M = M_r + J \omega', \quad (7)$$

(in which ω' is the derivative of the velocity with regard to time), taking into account (6) we will put the dependence of (5) in the form of the function on two variables ω_1 and ω

$$\Delta P_{en} \approx a \left(\frac{\Psi_m}{\omega_1} - \frac{T_r \Psi_m}{\omega_1^2} \omega_1' \right)^2 + \frac{b \cdot \omega_1^2}{\Psi_m^2} (M_r + J \cdot \omega')^2 + c \cdot \omega_1^{2-2} + d \cdot \omega^2. \quad (8)$$

Moreover, the difference between these variables ω_1 and ω , referred to the nominal value of the angular frequency of the

stator ω_{1n} , in the frequency control of the FRAE is called absolute slip

$$\beta = (\omega_1 - \omega) / \omega_{1n} = \omega_1 - \omega, \quad (9)$$

and may exceed, as shown below, when the SNS is several times the nominal slip of the FRAE.

For an exact calculation of the TMPL ΔP_{em} for the FRAE in the considered modes, we transform the dependence (8) (by eliminating the assumption made in (4) by introducing into the last but one term, according to (1), the correction factor k_ψ) into the form

$$\Delta P_{en} = a \left(\frac{\Psi_m}{\omega_1} - \frac{T_r \Psi_m}{\omega_1^2} \omega_1' \right)^2 + \frac{b \cdot \omega_1^2}{\Psi_m^2} (M_r + J \cdot \omega')^2 + k_\psi \cdot c \cdot \omega_1^{\lambda-2} + d \cdot \omega^2. \quad (10)$$

The coefficient k_ψ is calculated (taking into account (3) and the mentioned book by Pivnyak G.G.) in the form

$$\left. \begin{aligned} k_\psi &= \left(\frac{\Psi_m}{\Psi_{mn}} \right)^2 \left(\frac{\Psi_r}{\Psi_r} \right)^2; \quad I_{1xn} = \frac{\Psi_m}{L_m}; \quad I_{1yn} = \frac{M_n}{k_r \Psi_m} \\ \Psi_{mx} &= k_r (\Psi_r + L_{\sigma r} I_{1x}); \quad \Psi_{my} = k_r L_{\sigma r} I_{1y} \\ \Psi_{mx.n} &= k_r (\Psi_m + L_{\sigma r} I_{1x.n}); \quad \Psi_{my.n} = k_r L_{\sigma r} I_{1y.n} \\ \Psi_m^2 &= \Psi_{mx}^2 + \Psi_{my}^2; \quad \Psi_{mn}^2 = \Psi_{mx.n}^2 + \Psi_{my.n}^2 \end{aligned} \right\}, \quad (11)$$

where $L_{\sigma r}$ is the leakage inductance of the engine rotor; index "n" denotes the values related to the nominal mode of operation of the FRAE.

Based on (6, 7), we define (according to the book by Pivnyak G. G. and others) from the relationship

$$\beta = R_r \cdot M / \Psi_r^2 = \tau \cdot \omega_1^2, \quad \text{where} \quad \tau = R_r \cdot M / \Psi_m^2, \quad (12)$$

the current value of the absolute slip of the FRAE in the considered regime of acceleration or deceleration in the SNS. As follows from (12), the signs for absolute slip β and coefficient τ are determined by the sign of the developed electromagnetic torque M of the engine. With positive values of speed this sign is: positive – in the engine and negative – in the generator mode of the FRAE operation.

Substituting the first relation from (12) into expression (9), after equivalent transformations, we obtain an algebraic equation of the form

$$\omega_1^2 - \omega_1 / \tau + \omega / \tau = 0,$$

the solution for which is the dependency

$$\omega_1 = \left(1 - \sqrt{1 - 4 \cdot \tau \cdot \omega} \right) / 2\tau. \quad (13)$$

Substituting this solution in (12), we will find the calculated dependence for the absolute slip β of the FRAE in the considered regimes

$$\beta = \left(1 - \sqrt{1 - 4 \cdot \tau \cdot \omega} \right)^2 / 4\tau. \quad (14)$$

For the given tachogram $\omega(t)$ of the FRAE, taking into account (9, 14), we calculate the current value of the angular frequency $\omega_1(t)$ of the motor stator acceleration and braking modes, corresponding to the tachogram, for SNS

$$\omega_1(t) = \omega(t) + \beta. \quad (15)$$

Through the value ω of the rotor speed and the current value ω_1 of the stator frequency calculated from (15), the current TMPL values ΔP_{em} for the FRAE are calculated from (10), through which from the ratios in (2) the MEEL values ΔW_a and ΔW_d are found for this engine also in acceleration and braking modes.

At the second stage, we will determine the type of energy-saving paths of the FRAE speed ω for the SNS range under study in acceleration and braking modes at a constant value ($M_r = \text{const}$) of the static moment of the machine drive (using the example of the reverse motion of the main table drive for heavy metal-working longitudinal planing machine of 7B-220-6 type after carrying out the modernization in it, associated with the replacement of the DC motor on the FRAE).

By the energy-saving trajectory of the change of the speed of an FRAE, we will further understand this type of its change during acceleration or deceleration in the range of the SNS, which ensures minimization of the MEEL $\Delta W_a = \Delta W_a^o = \min$ and $\Delta W_d = \Delta W_d^o = \min$ for the SNS, calculated from dependencies (2). At the same time, it is known from the theory of variational calculus (for example, from the book by Andreeva V.A., Tsurulyova V.M. Variational calculus and optimization methods) that when minimizing the integrals from (2), the integrand function ΔP_{en} for them should follow the Euler equation for each variable in this function.

According to the above, we write the Euler equation for the TMPL ΔP_{en} function from (8) with reference to the variable in it ω

$$\frac{\partial^2(\Delta P_{en})}{\partial \omega' \cdot \partial \omega'} \cdot \omega'' + \frac{\partial^2(\Delta P_{en})}{\partial \omega \cdot \partial \omega'} \cdot \omega' + \frac{\partial^2(\Delta P_{en})}{\partial \omega \cdot \partial t} - \frac{\partial(\Delta P_{en})}{\partial \omega} = 0, \quad (16)$$

where ω'' is the second derivative of the speed with respect to time.

Substituting the value of the function ΔP_{en} from (8) into equation (16) and calculating (for $M_r = \text{const}$) the analytical expressions of partial derivatives for it, we transform, taking into account $\omega_1 \approx \omega$, the Euler equation (16) to the form

$$\omega'' \approx K / \omega, \quad \text{where} \quad K = d \cdot \Psi_m^2 / bJ^2. \quad (17)$$

The differential equation from (17) is non-linear and therefore, as is well known, it does not have an exact analytical solution. As follows from finding the exact solution of this equation using the Runge-Kutta method, for the considered initial and final conditions, it can be interpolated (with a relative standard deviation of less than 1.1 %) with energy-saving paths of the FRAE velocity, "Quasi-optimal":

of concave

$$\left. \begin{aligned} \omega &= \omega_n + (\omega_m - \omega_n) \cdot \frac{\text{sh}(\xi^* \sqrt{K} \cdot t)}{\text{sh}(\xi^* \sqrt{K} \cdot t_a)} \\ \omega &= \omega_n + (\omega_m - \omega_n) \cdot \frac{\text{sh}[\xi^* \sqrt{K} \cdot (t_a - t)]}{\text{sh}(\xi^* \sqrt{K} \cdot t_d)} \end{aligned} \right\}; \quad (18)$$

or convex shape

$$\left. \begin{aligned} \omega &= \omega_n + (\omega_m - \omega_n) \cdot \left\{ 1 - \frac{\text{sh}[\xi^* \sqrt{K} \cdot (t_a - t)]}{\text{sh}(\xi^* \sqrt{K} \cdot t_a)} \right\} \\ \omega &= \omega_n + (\omega_m - \omega_n) \cdot \left\{ 1 - \frac{\text{sh}(\xi^* \sqrt{K} \cdot t)}{\text{sh}(\xi^* \sqrt{K} \cdot t_d)} \right\} \end{aligned} \right\}. \quad (19)$$

The first dependences in (18, 19) correspond to the acceleration, and the second ones – to the deceleration.

In these dependencies, the value of the correction coefficient ξ^* corresponds to the minimum possible value from (2) MEEL for FRAE, found using the updated value (10) for the MEEL and accurate determination of the angular frequency ω_1 value in it.

According to the calculation results from (2, 10), the following relations are constructed in the form of graphs: in

Fig. 1 – the dependences of the MEEL ΔW_a , ΔW_d ; in Fig. 2, a – the change in the correction factor ξ^* for the FRAE – by varying the durations of the acceleration t_a and deceleration t_d time of the machine drive (with $M_r/M_n=0.2$) in the considered range of the SNS. In these and subsequent Figures, curves 1 and 2 refer to quasi-optimal tachograms, respectively, of concave and convex shapes, curves 3 and 4, to a parabolic type of tachograms, respectively, of concave and convex shapes, and curves 5, to linear tachograms.

For these durations of acceleration and deceleration time, Table 2 gives the MEEL values ΔW_a and ΔW_d calculated from (2) as well as the calculated specific energy losses Δp_a and Δp_d for the FRAE when moving α_a and α_d its rotor in these modes

$$\left. \begin{aligned} \Delta p_a &= \Delta W_a / \alpha_a; & \Delta p_d &= \Delta W_d / \alpha_d \\ \alpha_a &= \int_0^{t_a} \omega \cdot dt; & \alpha_d &= \int_0^{t_d} \omega \cdot dt \end{aligned} \right\} \quad (20)$$

At the third stage, we find the type of energy saving paths of FRAE speeds during acceleration and deceleration in the considered SNS range with respect to the electric traction drive

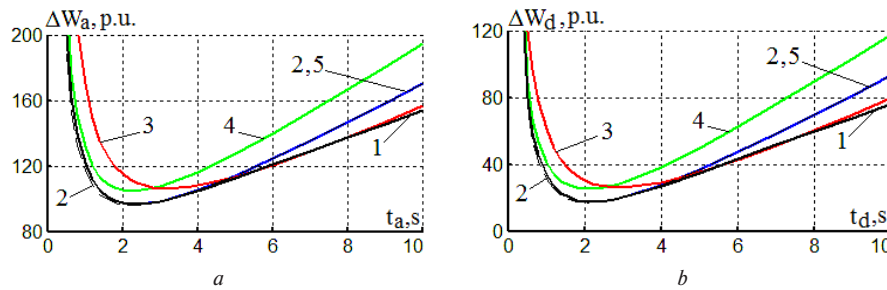


Fig. 1. Dependences of the MEEL ΔW_a , ΔW_d for FRAE in machine drive (for $M_r/M_n=0.2$) with varying durations of acceleration (a) and deceleration time (b) for:

1 and 2 – quasi-optimal concave and convex; 3 and 4 – parabolic concave and convex; 5 – linear tachograms

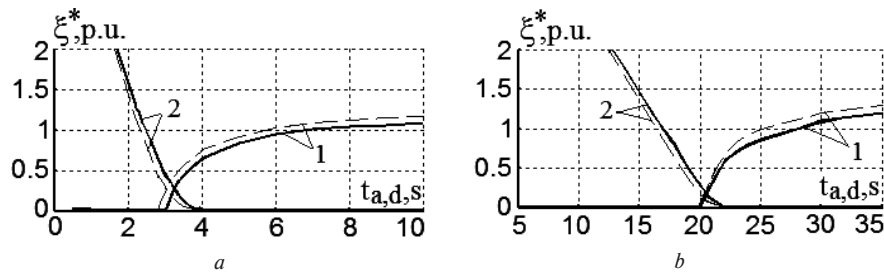


Fig. 2. Dependences $\xi^*(t_{a,d})$ for machine (a) and traction (b) drives:

1 – for concave and 2 – for convex quasi-optimal tachograms (solid line – during acceleration, dotted line – during deceleration)

Table 2

MEEL values ΔW_a , ΔW_d and specific energy losses Δp_a , Δp_d during acceleration and braking modes in machine (with $M_r/M_n=0.2$ and $t_a=t_d=4$ s) and traction (with $m=18.2$, $i=0.02$ and $t_a=t_d=25$ s) drives

Tachogram view	Values ΔW_a , ΔW_d , p. u. and Δp_a , Δp_d , p. u.							
	Machine drive (with $K=1.339 \cdot 10^{-6}$)				Traction drive (with $K=1.615 \cdot 10^{-8}$)			
	Acceleration		Deceleration		Acceleration		Deceleration	
Values ξ_1^* and ξ_2^*	$\xi_1^*=0.65, \xi_2^*=0.05$		$\xi_1^*=0.76, \xi_2^*=0.05$		$\xi_1^*=0.9, \xi_2^*=0.01$		$\xi_1^*=1.0, \xi_2^*=0.01$	
Magnitude	ΔW_a	Δp_a	ΔW_d	Δp_d	ΔW_a	Δp_a	ΔW_d	Δp_d
Quasi-opt. (concave)	104.8	0.0470	26.99	0.0120	543.4	0.0440	157.1	0.0126
Quasi-opt. (convex)	105.1	0.0438	27.53	0.0122	544.8	0.0431	159.1	0.0128
Parabolic (concave)	107.9	0.0552	29.13	0.0149	563.5	0.0510	172.6	0.0156
Parabolic (convex)	116.1	0.0456	38.44	0.0145	600.9	0.0422	214.3	0.0150
Linear	105.1	0.0438	27.53	0.0122	544.8	0.0431	159.1	0.0128

shaft; m is the total mass of the trolley, kg; η_m is the coefficient of performance (efficiency) of the driving mechanism of the trolleybus, %; α and i are respectively, the angle of ascent/descent [deg] and longitudinal slope, %; $g = 9.81$ m/s² is acceleration of free fall; $\gamma = (1.15-1.2)$ is the coefficient taking into account the reduction of the kinetic energy of all rotating parts of the traction drive (wheel sets, mechanical couplings, gears of the gearbox, propeller shaft and the engine rotor) to an equivalent mass equal $m(1 + \gamma)$ to the forward movement of the trolleybus.

We write the kinetic energy of a moving trolleybus in the form of two equivalent expressions

$$\left. \begin{aligned} W_k &= 0.5m(1 + \gamma) \cdot v^2 [\text{m/s}] \\ W_k &= 0.5J \cdot \omega^2 [\text{rad/s}] = 0.5J \cdot \varepsilon^2 \cdot v^2 [\text{m/s}] \end{aligned} \right\}, \quad (22)$$

where the first corresponds to the reduction of all moving parts of the drive train to the forward movement, and the second – to the reduction of all translational and rotationally moving parts of the drive to the engine shaft. Equating to each other the equalities of (22), we determine the value of the moment of inertia of the trolleybus drive reduced to the shaft of the traction engine

$$J = m(1 + \gamma) \cdot v^2 [\text{m/s}] / \omega^2 [\text{rad/s}] = m(1 + \gamma) / \varepsilon^2. \quad (23)$$

After transferring of the absolute values ω , M_r and J calculated from (21, 23) from the absolute system of units to the relative one and their subsequent substitution into expressions (8, 10), it becomes possible to determine the current values of the MEEL for FRAE in acceleration and braking modes in the SNS range from these expressions. In comparison with the previously considered constant load applied to the machine drive, the traction drive feature, taking into account (21), is the variable value of its resistance moment M_r from the slope i of the roadbed and the speed rotor ω of the FRAE

$$\left. \begin{aligned} M_r &= M_{r0} + q \cdot \omega^2; \quad \omega = \varepsilon \cdot v [\text{m/s}] / \omega_b \\ M_{r0} &= \frac{mg(0.012 + i)}{\varepsilon \eta_m M_b}; \quad q = \frac{5.184 \cdot 10^{-5} mg \omega_b^2}{\varepsilon^3 \eta_m M_b} \end{aligned} \right\}, \quad (24)$$

where M_b and $\omega_b = 100\pi/z_p$ are the basic values of the electromagnetic moment [Nm] and the rotor speed [rad/s] of the engine, respectively; z_p is the number of pairs of fields of the engine (for the considered FRAE: $z_p = 2$); $\eta_m = 92.8$ % is the average efficiency of the trolleybus driving mechanism (according to the book by Rosenfeld V.E. and others, its current value for a trolleybus varies depending on the load from 89.8 to 95.8 %). The values ω , M_r , M_{r0} and q are given in (24) in relative units, and the values of m and ε – in kg and rad/m respectively. For the maximum mass of the trolleybus and the longitudinal axis equal to 2 %, the following values correspond: $M_{r0} = 0.2743$ and $q = 0.01736$ p. u.

From (24), the dependence of the static moment M_r of the FRAE on the values of the speeds of the trolleybus v and the engine ω were calculated in the SNS range and plotted in Fig. 3 in the form of graphs. Substituting the value for the moment of resistance M_r from (24) into expression (8), and then

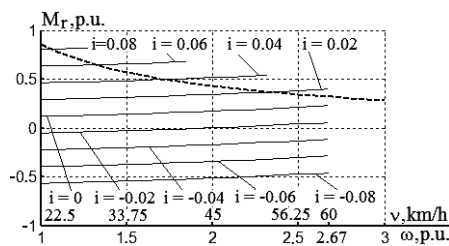


Fig. 3. Static load characteristics of the FRAE under SNS for traction drive (bold dotted line shows dependency: $\omega M_r = P_n$)

this expression into equation (16), we transform the last expression obtained taking into account $\omega_1 \approx \omega$ the form

$$\omega'' \approx K/\omega + 2M_{r0}q\omega/J^2 + 2q^2\omega^3/J^2. \quad (25)$$

Due to the nonlinear form of the obtained second-order differential (25), it does not have an exact analytical solution. As research studies of the exact solutions of this equation obtained by the Runge-Kutta method showed, they can be interpolated (with a standard deviation of less than 0.6 %) with analytical dependencies (18, 19) in the form of temporary functions of the hyperbolic sinus, containing the correction factor ξ^* in their arguments, minimizing the values of the MEEL for the FRAE for any given value of the durations of time t_a and t_d . Graphic dependencies for the coefficient ξ^* are shown for Fig. 2, b.

For traction load (at $m = 18.2t$, $i = 0.02$, $v_m = 50$ km/h and durations of acceleration t_a and deceleration t_d time of FRAE, equal to 25 s) there are calculated from dependencies (3, 7, 11, 14, 15, 18, 19, 23 and 24) transient electromechanical processes (speed ω , absolute slip β , rotor flow coupling module Ψ_r , electromagnetic moment M , module of generalized stator current vector I_1 , coefficient k_ψ) and calculated from expressions (2, 10) transient energy processes (total main power ΔP_{en} and energy losses ΔW_a , ΔW_d), which are shown in Fig. 4.

For the indicated durations of the acceleration and deceleration times, the values ΔW_a , ΔW_d of the MEEL and the specific energy losses calculated by relations (20) Δp_a and Δp_d FRAE are presented in Table 2. According to the results, the calculations from (2, 10) are plotted in Fig. 5 for the MEEL graphs for this FRAE with traction load for the durations of acceleration t_a and deceleration t_d time.

At the fourth stage, we analyze the data from Tables 2 and 3, the graphs in Figs. 1, 4 and 5:

- the smallest values of MEEL during acceleration and deceleration of the FRAE in the SNS range are inherent in the quasi-minimal tachograms (TG): convex (at $t_{a,d} \leq t_{a,d}^o$) or concave (at $t_{a,d} > t_{a,d}^o$) shape, where $t_{a,d}^o$ are optimal (Table 3) values of acceleration (deceleration) time, corresponding to the minimum value of the MEEL for the FRAE; moreover, we note that with $t_{a,d} > t_{a,d}^o$ a quasi-optimal TG of a convex shape, it virtually coincides with the linear TG;

- parabolic and quasi-optimal TG of a concave form may not be applicable in practice during acceleration of the FRAE because of the incomparably high values of the motor's stator current (with this taken into account, the smallest MEELs during acceleration are actually achieved due to quasi-optimal convex or linear tachograms);

- the smallest values of the stator current during acceleration are characteristic of a parabolic TG of a convex shape (which in this regime always has the highest values of MEEL among all considered types of TG);

- under deceleration regimes, all investigated types of TG are applicable for FRAE (with the lowest values of MEEL and engine stator current inherent in a quasi-optimal TG of a concave shape, and the largest – a parabolic TG of convex shape).

For the transition in quantitative assessment of electromechanical and energy processes from relative to absolute values, the values obtained in relative units should be multiplied by the corresponding basic values presented for the FRAE in Table 4.

Conclusions.

1. The energy saving (called “quasi-optimal”) trajectories of the FRAE speed trajectory in the range of super-nominal speeds obtained in the form of dependences (18, 19) minimize the total main energy losses of this engine in acceleration and braking modes with constant and traction loads. At the same time, in the specified speed range, the transition from the known parabolic type of trajectories of speed to the quasi-op-

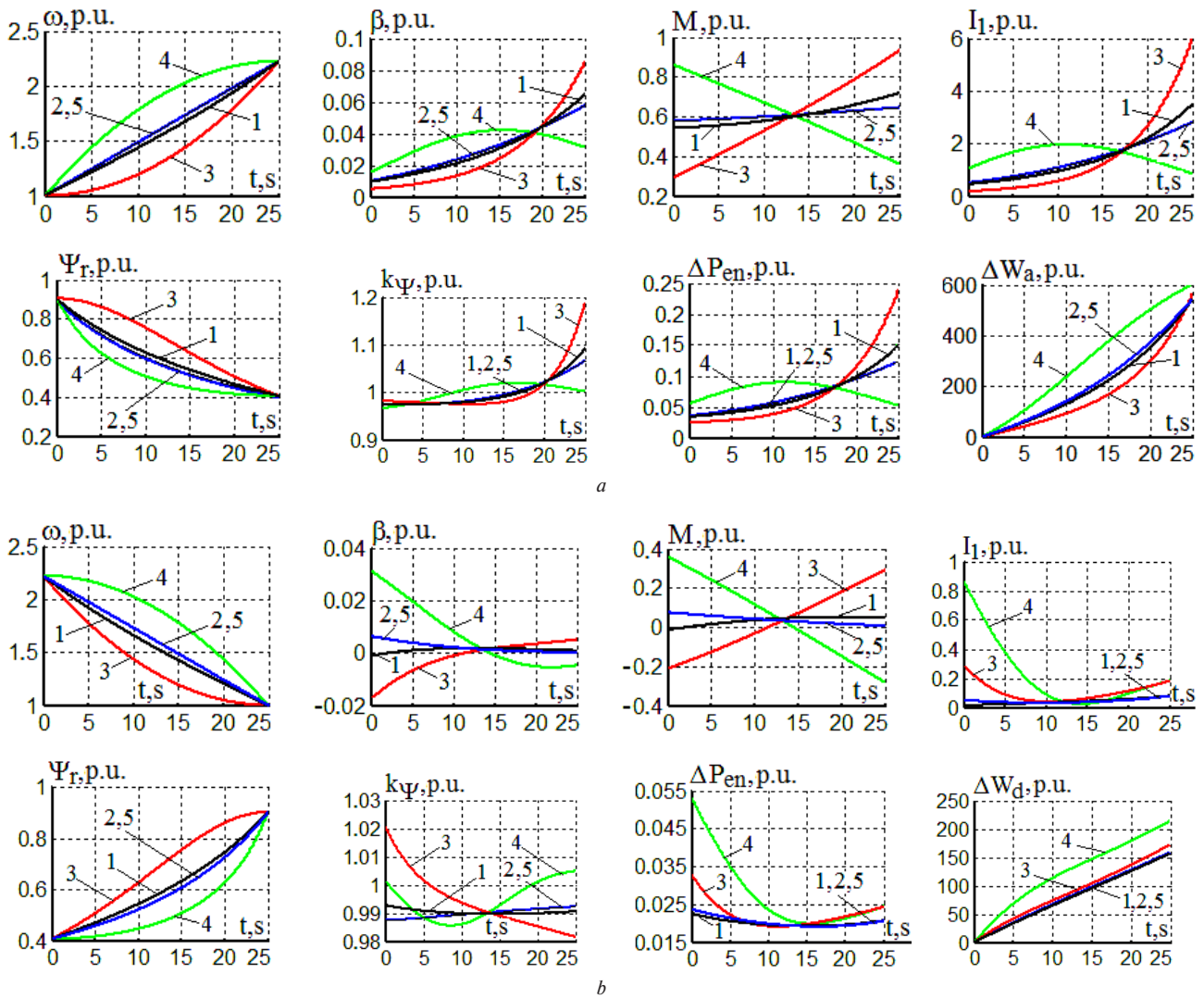


Fig. 4. Electromechanical and energy transients of the FRAE in the traction drive (for $t_a = t_d = 25$ s, $m = 18.2t$, $i = 0.02$, $v_m = 50$ km/h) during acceleration (a) and deceleration (b) for:

1 and 2 – quasi-optimal concave and convex; 3 and 4 – parabolic concave and convex; 5 – linear tachograms

Table 3

Values of optimal time $t_{a,d}^o$ and MEEL ΔW_a^o , ΔW_d^o for FRAE, corresponding to Figs. 1, a, b and Figs. 5, a, b

Number of Figs.	Number of curves	t_a^o	t_d^o	ΔW_a^o	ΔW_d^o
	units	s	s	p.u.	p.u.
1, a, b (machine drive)	1.5	2.36	2.19	96.50	17.51
	2	2.25	2.12	96.00	17.12
	3	3.22	2.90	106.2	26.09
	4	2.27	2.08	104.8	25.13
5, a, b (traction drive)	1.5	14.7	13.8	498.3	106.7
	2	14.2	13.4	496.0	105.2
	3	19.5	17.8	551.7	154.2
	4	14.7	13.5	545.3	149.9

timal trajectory allows (for example, traction drive) saving losses of engine energy from 4 to 10 % – when accelerating or from 9 to 27 % – when deceleration.

2. For the first time, the obtained analytical dependencies (13, 14) make it possible to determine the current values of the absolute slip β and stator angular frequency ω_1 while weakening the magnetic field of the FRAE in the

modes of its acceleration and deceleration at super nominal speeds.

3. The proposed dependences from (24) allow calculating the static load characteristic $M_r(\omega)$ of the traction engine through the mass load and speed of the trolleybus, the slope of the roadway, whereas the third ratio from (21) allows finding traction force F_r of the trolleybus through the current value of the engine moment M .

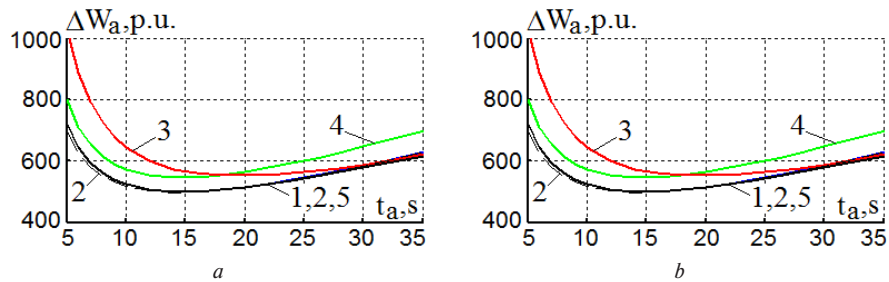


Fig. 5. Dependences of the MEEL ΔW_a value for the FRAE with traction load at varying the durations of acceleration (a) and deceleration time (b) for:

1 and 2 – quasi-optimal concave and convex; 3 and 4 – parabolic concave and convex; 5 – linear tachograms

Table 4

Basic values of engine magnitudes

Magnitude	I_1	M, M_r	Ψ	ω_1	ω	$P, \Delta P$	ΔW	R_s, R_r	L	J	t
Dimension	A	Nm	WB	rad/s	rad/s	kW	J	Om	mH	kg·m ²	s
Values	286.4	893	1.039	100π	50π	140.27	446.4	1.1402	3.65	0,0181	0.01/π

4. “U”-shaped type of MEEL dependencies for the FRAE on the durations of acceleration and deceleration times in the SNS range is determined (according to Figs. 1 and 5), which indicates the presence of certain values of the durations of acceleration and deceleration time, at which these losses are minimal for all researched types (linear, parabolic and quasi-optimal) of speed trajectories. With energy saving (quasi-optimal and linear) speed trajectories, the transition to optimal lengths of acceleration and deceleration time allows, in the SNS range, decreasing MEEL values additionally for the FRAE with traction load (by 20 % during acceleration and by 50 % during deceleration).

5. It was revealed (according to Table 2) that the smallest ratios Δp_a and Δp_d from (20) between MEEL ΔW_a , ΔW_d and movements α_a , α_d of the shaft of the FRAE (the latter are directly proportional to the movement of the trolleybus) are characterized: during acceleration – by a quasi-optimal convex shape and linear TG, and when decelerating – by quasi-optimal concave shape TG.

References.

- Zhang, X., Yu, Y., Zhang, G., Zhang, J., Wang, B., & Xu, D. (2018). Maximum Torque Increase and Performance Optimization for Induction Motor Field-Weakening Control. *IEEE ICEMS*, 1268-1272. DOI: 10.23919/ICEMS.2018.8548976.
- Harikrishnan, P., Jose, T., Kamalesh, H., & Eswara, S.R. (2017). Effect of Stator Leakage Inductance in Field Weakening Region of a Vector Controlled Induction Machine Drive for Traction Application. *IEEE ITEC-India*, 841-846. DOI: 10.1109/ITEC-India.2017.8356940.
- Nguyen-Thac, K., Orlowska-Kowalska, T., & Tarchala, G. (2012). Comparative analysis of the chosen field-weakening methods for the Direct Rotor Flux Oriented Control drive system. *Archives of electrical engineering*, 61(4), 443-454. DOI: 10.2478/v10171-012-0038-7.
- Su, J., Gao, R., & Husain, I. (2017). Model Predictive Control based Field-weakening Strategy for Traction EV used Induction Motor. *IEEE Transactions on Industry Applications*, 2295-2305. DOI: 10.1109/TIA.2017.2787994.
- Aswathy, M. S., & Beevi, M. W. (2015). High Performance Induction Motor Drive in Field Weakening Region. *IEEE ICCS*, 242-247. DOI: 10.1109/ICCS.2015.7432899.
- Ebbesen, S., Salazar, M., Elbert, Ph., Bussi, C., & Onder, C.H. (2017). Time-optimal Control Strategies for a Hybrid Electric Race Car. *IEEE Transactions on Control Systems Technology*, 233-247. DOI: 10.1109/TCST.2017.2661824.
- Haahr, J. T., Pisinger, D., & Sabbaghian, M. (2017). A dynamic programming approach for optimizing train speed pro-

- files with speed restrictions and passage points. *Transportation Research Part B*, (99), 167-782. DOI: 10.1016/j.trb.2016.12.016.
- Lu, Sh., Hillmansen, St., Ho, T. K., & Roberts, C. (2013). Single-Train Trajectory Optimization. *IEEE Transactions on Intelligent Transportation Systems*, 14(2), 743-750. DOI: 10.1109/TITS.2012.2234118.
- Xiao, Zh., Sun, P., Wang, Q., Zhu, Y., & Feng, X. (2018). Integrated Optimization of Speed Profiles and Power Split for a Tram with Hybrid Energy Storage Systems on a Signalized Route. *Energies*, (11), 1-21. DOI: 10.3390/en11030478.
- Volkov, A. V., & Kolesnikov, A. A. (2013). Energy-saving speed control of variable frequency asynchronous engine in acceleration and deceleration regimes. *Electronika*, (5), 2-9.

Енергозберігаючі тахограми розгону (гальмування) частотно-регульованого асинхронного двигуна

В. О. Волков

Національний технічний університет „Дніпровська політехніка“, м. Дніпро, Україна, e-mail: green_stone@ukr.net

Мета. Знаходження для діапазону сверхномінальних швидкостей короткозамкненого частотно-регульованого асинхронного двигуна енергозберігаючих траєкторій швидкості в режимах розгону й гальмування та дослідження загальних втрат енергії зазначеного двигуна в цих режимах на прикладі верстатного й тягового приводів.

Методика. Використані методи: варіаційного числення, Рунге-Кутта, математичної інтерполяції та комп'ютерного моделювання.

Результати. Отримані аналітичні залежності для розрахунку загальних втрат енергії для частотно-регульованого асинхронного двигуна (ЧРАД) за режимів розгону й гальмування в діапазоні його сверхномінальних швидкостей. Виконана кількісна оцінка цих втрат енергії для даного двигуна в зазначеному діапазоні швидкостей стосовно до постійного й тягового навантажень для запропонованої енергозберігаючої та відомих (лінійного й параболічного виду) траєкторій швидкості. Досліджені електромеханічні та енергетичні перехідні процеси ЧРАД у діапазоні сверхномінальних швидкостей для режимів розгону й гальмування з тяговим навантаженням.

Наукова новизна. Уперше запропонована енергозберігаюча (названа „квазіоптимальною“) траєкторія зміни

швидкості ЧРАД при сверхномінальних швидкостях, що дозволяє мінімізувати загальні основні втрати енергії двигуна в режимах розгону й гальмування з постійним і тяговим навантаженнями. Уперше виконана кількісна оцінка мінімально можливих загальних основних втрат енергії цього двигуна в режимах розгону й гальмування в діапазоні сверхномінальних швидкостей для запропонованої енергозберігаючої траєкторії швидкості та порівняння цих втрат з лінійною й параболічною тахограмами.

Практична значимість. Використання отриманих результатів дозволяє зменшити непродуктивні втрати енергії в режимах розгону й гальмування ЧРАД при сверхномінальних швидкостях з постійним і тяговим навантаженнями.

Ключові слова: частотне регулювання, асинхронний двигун, сверхномінальна швидкість, енергозбереження

Энергосберегающие тахограммы разгона (торможения) частотно-регулируемого асинхронного двигателя

В. А. Волков

Национальный технический университет „Днепровская политехника“, г. Днепр, Украина, e-mail: green_stone@ukr.net

Цель. Нахождение для диапазона сверхномінальных скоростей короткозамкнутого частотно-регулируемого асинхронного двигателя энергосберегающих траекторий скорости в режимах разгона и торможения и исследование общих потерь энергии указанного двигателя в этих режимах на примере станочного и тягового приводов.

Методика. Используются методы: вариационного исчисления, Рунге-Кутта, математической интерполяции и компьютерного моделирования.

Результаты. Получены аналитические зависимости для расчета общих потерь энергии для частотно-регулируемого асинхронного двигателя (ЧРАД) при режимах разгона и торможения в диапазоне его сверхномінальных скоростей. Выполнена количественная оценка этих потерь энергии для данного двигателя в указанном диапазоне скоростей применительно к постоянной и тяговой нагрузкам для предложенной энергосберегающей и известных (линейного и параболического вида) траекторий скорости. Исследованы электромеханические и энергетические переходные процессы ЧРАД в диапазоне сверхномінальных скоростей для режимов разгона и торможения с тяговой нагрузкой.

Научная новизна. Впервые предложена энергосберегающая (названная „квазиоптимальной“) траектория изменения скорости ЧРАД при сверхномінальных скоростях, позволяющая минимизировать общие основные потери энергии двигателя в режимах разгона и торможения с постоянной и тяговой нагрузками. Впервые выполнена количественная оценка минимально возможных общих основных потерь энергии этого двигателя в режимах разгона и торможения в диапазоне сверхномінальных скоростей для предложенной энергосберегающей траектории скорости и сравнение этих потерь с линейной и параболической тахограммами.

Практическая значимость. Использование полученных результатов позволяет уменьшить непроизводительные потери энергии в режимах разгона и торможения ЧРАД при сверхномінальных скоростях с постоянной и тяговой нагрузками.

Ключевые слова: частотное регулирование, асинхронный двигатель, сверхномінальная скорость, энергосбережение

Рекомендовано до публікації докт. техн. наук С. М. Тиховодом. Дата надходження рукопису 02.08.18.